Hamdullah Yücel   Martin Stoll   Peter Benner

Discontinuous Galerkin Finite Element Methods with Shock-Capturing for Nonlinear Convection Dominated Models

Max Planck Institute Magdeburg
Preprints

Abstract

In this paper, convection-diffusion-reaction models with nonlinear reaction mechanisms, which are typical problems of chemical systems, are studied by using the upwind symmetric interior penalty Galerkin (SIPG) method. The local spurious oscillations are minimized by adding an artificial viscosity diffusion term to the original equations. A discontinuity sensor is used to detect the layers where unphysical oscillations occur. Finally, the proposed method is tested on various single- and multi-component problems.

Contents

Author's addresses:

Hamdullah Yücel, Martin Stoll, Peter Benner
Computational Methods in Systems and Control Theory, Max Planck Institute
for Dynamics of Complex Technical Systems, Sandtorstr. 1, 39106 Magdeburg
Germany, ({yuecel,stollm,benner}@mpi-magdeburg.mpg.de)

1. Introduction

Unsteady nonlinear convection diffusion reaction problems are often studied in many engineering problems such as fluid dynamics problems in the presence of body forces, electrochemical interaction flows and chemically reactive flows [11, 12]. In this paper, we consider the following nonlinear system of coupled diffusion-convection-reaction equations as a model problem for our investigations:

$$\partial_t u_i - \varepsilon_i \Delta u_i + \beta_{\mathbf{i}} \cdot \nabla u_i + \alpha_i u_i + r_i(\mathbf{u}) = f_i \qquad \text{in} \quad \Omega_i, \qquad (1.1a)$$

$$u_i = g_i^D \qquad \text{on} \quad \Gamma_i^D, \qquad (1.1b)$$

$$\varepsilon \frac{\partial u_i}{\partial n} = g_i^N \qquad \text{on} \quad \Gamma_i^N, \qquad (1.1c)$$

$$u_i(\cdot, t_0) = u_i^0 \qquad \text{in} \quad \Omega_i \qquad (1.1d)$$

for $i = 1, \cdots, m$. Here, $\mathbf{u} = \mathbf{u}(\mathbf{x}, t)$ with $\mathbf{u} = (u_1, \cdots, u_m)^T$ denotes the vector of unknowns where Ω_i is a bounded, convex domain in $\mathbb{R}^2$ with boundary $\Gamma_i = \overline{\Gamma_i^D \cup \Gamma_i^N}$, $\Gamma_i^D \cap \Gamma_i^N = \emptyset$ and $t \in (0, T]$ for some $T > 0$. The source functions and boundary conditions, i.e., Dirichlet boundary condition (1.1b) and Neumann boundary condition (1.1c), are defined such as $f_i \in L^2(0, T; L^2(\Omega))$, $g_i^D \in L^2(0, T; H^{3/2}(\Gamma_i^D))$ and $g_i^N \in L^2(0, T; H^{1/2}(\Gamma_i^N))$, respectively. Moreover, the diffusion coefficients ε_i are small positive numbers such that $0 < \varepsilon_i \ll 1$, $\alpha_i \in L^\infty(\Omega)$ are the reaction coefficients and $\beta_i \in L^\infty(0, T; (W^{1,\infty}(\Omega))^2)$ are the velocity fields (see Appendix A for the definitions of functional and Sobolev spaces). The initial conditions are also defined such that $u_i^0 \in H^1(\Omega)$. We have the following assumptions for the nonlinear reaction parameter $r(\mathbf{u})$:

$$r(\mathbf{u}) \in C^1(\mathbb{R}_0^+), \quad r(0) = 0, \quad r'(s) \geq 0 \quad \forall s \geq 0, \quad s \in \mathbb{R}. \qquad (1.2)$$

to satisfy the boundedness of $r'(u)$ in terms of above compact intervals of u. In large chemical systems the reaction terms $r(\mathbf{u})$ are assumed to be expressions which are products of some function of the concentrations of the chemical component and an exponential function of the temperature, called Arrhenius kinetics expression. As an example, the rate of conversion of u_1 and u_2 in the reaction

$$u_1 + u_2 \rightarrow \text{ products}$$
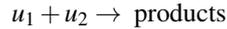
can be expressed as

$$k_0 u_1^a u_2^b e^{-\frac{E}{\mathcal{R}T}},$$

where u_1 and u_2 are the concentrations of reactants, a and b are the orders of reaction, k_0 is the preexponential factor, E is the activation energy, $\mathcal{R}$ is the universal gas constant and T is the absolute reaction temperature.

Problems of the form (1.1) are strongly coupled such that inaccuracies in one unknown directly affect all other unknowns. Prediction of these unknowns is very important for the safe and economical operation of biochemical and chemical engineering processes. Typically, in (1.1) the size of the diffusion parameter ε is smaller compared to the size of velocity field β. Then, such a convection diffusion system is called convection-dominated.

For convection-dominated problems, especially in the presence of boundary and/or interior layers, the standard finite element methods may result in spurious oscillations causing in turn a severe loss of accuracy and stability. To avoid these oscillations, some stabilization techniques are applied such as the streamline upwind Galerkin method (SUPG) for single linear convection dominated equations [14]. Nevertheless, spurious localized oscillations, in particular in cross-wind direction, may still be present. Recently, higher order discontinuous Galerkin (DG) methods have become popular for convection dominated problems [5, 8] since DG methods possess inherent stability at discontinuities. However, the stability condition sometimes is not satisfied by the DG space discretization itself at discontinuities and therefore, numerical solutions might suffer from unphysical oscillations near the discontinuities.

The most straightforward approach consists in avoiding the presence of sharp gradients with some non-linear projection operators, namely slope limiters, introduced in [6, 7]. Nevertheless, these limiters are not suitable for higher-order reconstructions, i.e., they drastically reduce the order of the approximation to linear or constant. Alternatively, a high-order reconstruction scheme, known as weighted non-oscillatory approach is used in [17] as a slope limiter. However, it requires structured grids with a very wide stencil and therefore the compactness of DG may become less attractive. In addition, the extension to multiple dimensions is still an open issue for both slope limiters. Another classical way to avoid spurious oscillations is the artificial viscosity proposed in [22], which is used with in many numerical techniques, i.e., finite difference methods [15], SUPG discretization [14] for linear convection dominated problems and in [1, 3] for nonlinear convection dominated problems. Within the DG framework, it is mostly used for Euler equations [16] as an alternative to slope limiters.

In this paper, we solve the convection dominated problems with various nonlinear reaction terms by using the upwind symmetric interior penalty Galerkin (SIPG) method. If necessary, we use a shock-capturing method proposed in [16] based on the element size and the polynomial degree in order to prevent unphysical oscillations. It is used in conjuction with a discontinuity detection strategy.

The rest of the paper is organized as follows: In the next section we introduce the model problem as scalar convection dominated reaction-diffusion equation with nonlinear reaction term. Section 3 specifies the upwind SIPG discretization in space with shock-capturing and time discretization. In the final section we present numerical results that illustrate the performance of discontinuous Galerkin approximation with shock-capturing.

2. Scalar equation as model problem

We use the following scalar equation as a model problem

$$\partial_t u - \varepsilon \Delta u + \beta \cdot \nabla u + \alpha u + r(u) = f \qquad \text{in} \quad \Omega, \tag{2.1}$$

equipped with appropriate initial and boundary conditions, i.e., Dirichlet and Neumann boundary conditions, to make the notation easier for the readers. Let us first consider the weak formulation of the state equation (2.1). The state space and the space of the test functions are

$$U = \{u \in H^1(\Omega) : u = g_D \text{ on } \Gamma_D\} \quad \text{and} \quad V = H_0^1(\Omega),$$

respectively. Then, it is well known that the weak formulation of the state equation (2.1) is

such that [9]

$$(\partial_t u, v) + a(u,v) + \int_\Omega r(u)v\,dx = l(v), \qquad \forall v \in V,$$

where

$$a(u,v) = \int_\Omega \left(\varepsilon \nabla u \cdot \nabla v + \beta \cdot \nabla uv + \alpha uv\right) dx, \quad l(v) = \int_\Omega fv\,dx + \int_{\Gamma_N} g_N v\,ds.$$

When shock-capturing is applied, we add an artificial viscosity $\left(\nabla \cdot (\mu \nabla u)\right)$ to the weak formulation of the problem (2.1). It is an unphysical diffusion term whose sole purpose is to damp out high frequency components of the solution encountered wherever Gibbs phenomenas are present. Then, the weak formulation with the artificial viscosity is given by

$$(\partial_t u, v) + a(u,v) + \int_\Omega r(u)v\,dx + \int_\Omega \nabla \cdot (\mu \nabla u)v\,dx = l(v), \qquad \forall v \in V,$$

where μ is the amount of viscosity. The viscosity parameter μ is chosen as a function of the mesh size and order of approximating polynomials. It will be described in Section 3.2 in more details.

3. Discretization Scheme

3.1. DG discretization in space

The DG discretization here is based on the SIPG discretization for the diffusion and the upwind discretization for the convection. The same discretization is used, e.g., in [13, 19] for scalar linear convection diffusion equations. In this paper, we follow the notation in [19].

Let $\{\mathcal{T}_h\}_h$ be a family of shape regular meshes such that $\overline{\Omega} = \cup_{K \in \mathcal{T}_h}\overline{K}$, $K_i \cap K_j = \emptyset$ for $K_i, K_j \in \mathcal{T}_h$, $i \neq j$. The diameter of an element K and the length of an edge E are denoted by h_K and h_E, respectively.

For an integer ℓ and $K \in \mathcal{T}_h$ let $\mathbb{P}^\ell(K)$ be the set of all polynomials on K of degree at most ℓ. We define the discrete state and test spaces to be

$$V_h = U_h = \left\{ u \in L^2(\Omega) : u\,|_K \in \mathbb{P}^\ell(K) \quad \forall K \in \mathcal{T}_h \right\}. \tag{3.1}$$

Note that since discontinuous Galerkin methods impose boundary conditions weakly, the space Y_h of discrete states and the space of test functions V_h are identical.

We split the set of all edges $\mathcal{E}_h$ into the set $\mathcal{E}_h^0$ of interior edges, the set $\mathcal{E}_h^D$ of Dirichlet boundary edges and the set $\mathcal{E}_h^N$ of Neumann boundary edges so that $\mathcal{E}_h = \mathcal{E}_h^\partial \cup \mathcal{E}_h^0$ with $\mathcal{E}_h^\partial = \mathcal{E}_h^D \cup \mathcal{E}_h^N$. Let n denote the unit outward normal to $\partial\Omega$. We define the inflow boundary

$$\Gamma^- = \{x \in \partial\Omega : \beta \cdot \mathbf{n}(x) < 0\},$$

and the outflow boundary $\Gamma^+ = \partial\Omega \setminus \Gamma^-$. The boundary edges are decomposed into edges $\mathcal{E}_h^- = \left\{E \in \mathcal{E}_h^\partial : E \subset \Gamma^-\right\}$ that correspond to inflow boundary and edges $\mathcal{E}_h^+ = \mathcal{E}_h^\partial \setminus \mathcal{E}_h^-$ that correspond to outflow boundary.

The inflow and outflow boundaries of an element $K \in \mathcal{T}_h$ are defined by

$$\partial K^- = \{x \in \partial K : \beta \cdot \mathbf{n}_K(x) < 0\}, \quad \partial K^+ = \partial K \setminus \partial K^-,$$

where $\mathbf{n}_K$ is the unit normal vector on the boundary ∂K of an element K.

Let the edge E be a common edge for two elements K and K^e. For a piecewise continuous scalar function u, there are two traces of u along E, denoted by $u|_E$ from inside K and $u^e|_E$ from inside K^e (see Figure 1). Then, the jump and average of y across the edge E are defined by:

$$[\![u]\!] = u|_E \mathbf{n}_K + u^e|_E \mathbf{n}_{K^e}, \quad \{\!\{u\}\!\} = \frac{1}{2}\left(u|_E + u^e|_E\right). \tag{3.2}$$

$$E$$
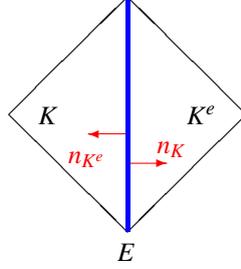
Figure 1: The edge E is a common edge for two elements K and K^e with unit outward normal vectors, $\mathbf{n}_K$ and $\mathbf{n}_{K^e}$.

Similarly, for a piecewise continuous vector field ∇u, the jump and average across an edge E are given by

$$[\![\nabla u]\!] = \nabla u|_E \cdot \mathbf{n}_K + \nabla u^e|_E \cdot \mathbf{n}_{K^e}, \quad \{\!\{\nabla u\}\!\} = \frac{1}{2}\left(\nabla u|_E + \nabla u^e|_E\right). \tag{3.3}$$

For a boundary edge $E \in K \cap \Gamma$, we set $\{\!\{\nabla u\}\!\} = \nabla u$ and $[\![u]\!] = u\mathbf{n}$ where $\mathbf{n}$ is the outward normal unit vector on Γ.

We can now give DG discretizations of the equation (2.1) in space. The DG method proposed here is based on the upwind discretization for the convection term and on the SIPG discretization for the diffusion term (see, e.g., [19]). This leads to the the following formulation:

$$(\partial_t u_h, v_h) + a_h(u_h, v_h) + \sum_{K \in \mathcal{T}_h} \int_K r(u_h) v_h \, dx = l_h(v_h) \quad \forall v_h \in V_h, \quad t \in (0, T], \tag{3.4}$$

where the (bi)-linear terms are defined as

$$\begin{aligned}
a_h(u, v) \quad &= \quad \sum_{K \in \mathcal{T}_h} \int_K \varepsilon \nabla u \cdot \nabla v \, dx \\
&\quad - \sum_{E \in \mathcal{E}_h^0 \cup \mathcal{E}_h^D} \int_E \{\!\{\varepsilon \nabla u\}\!\} \cdot [\![v]\!] \, ds - \sum_{E \in \mathcal{E}_h^0 \cup \mathcal{E}_h^D} \int_E \{\!\{\varepsilon \nabla v\}\!\} \cdot [\![u]\!] \, ds \\
&\quad + \sum_{E \in \mathcal{E}_h^0 \cup \mathcal{E}_h^D} \frac{\sigma \varepsilon}{h_E} \int_E [\![u]\!] \cdot [\![v]\!] \, ds + \sum_{K \in \mathcal{T}_h} \int_K \beta \cdot \nabla u v + \alpha u v \, dx \\
&\quad + \sum_{K \in \mathcal{T}_h} \int_{\partial K^- \backslash \Gamma^-} \beta \cdot \mathbf{n}(u^e - u) v \, ds - \sum_{K \in \mathcal{T}_h} \int_{\partial K^- \cap \Gamma^-} \beta \cdot \mathbf{n} u v \, ds, \tag{3.5}
\end{aligned}$$

4

$$l_h(v) = \sum_{K \in \mathcal{T}_h} \int_K f v \, dx + \sum_{E \in \mathcal{E}_h^D} \frac{\sigma \varepsilon}{h_E} \int_E g_D \mathbf{n} \cdot [\![v]\!] \, ds - \sum_{E \in \mathcal{E}_h^D} \int_E g_D \{\!\{\varepsilon \nabla v\}\!\} \, ds$$

$$- \sum_{K \in \mathcal{T}_h} \int_{\partial K^- \cap \Gamma^-} \beta \cdot \mathbf{n} \, g_D v \, ds + \sum_{E \in \mathcal{E}_h^N} g_N v \, ds, \tag{3.6}$$

with the nonnegative real parameter σ being a penalty parameter. We choose σ to be sufficiently large, independently of the mesh size h and the diffusion coefficient ε to ensure the stability of the DG discretization as described in [18, Sec. 2.7.1] with a lower bound depending only on the polynomial degree. Large penalty parameters decrease the jumps across element interfaces, which can affect the numerical approximation. However, the DG approximation can converge to the continuous Galerkin approximation as the penalty parameter goes to infinity (see, e.g., [4] for details).

3.2. DG Approximation with shock-capturing

Discontinuous Galerkin (DG) discretizations exhibit a better convergence behavior for convection dominated problems since they inherit stability at discontinuities [5, 8]. Nevertheless, spurious localized oscillations may still exist at discontinuities. These artifacts can cause unphysical negative values of concentrations of chemical species and lead to completely wrong predictions in complex chemical systems [2]. Therefore, as the DG solution develops, it has to be limited to prevent oscillations. A remedy is adding an artificial viscosity (a_{sc}, l_{sc}) to spread the discontinuity over a length scale. Then, the general scheme of shock-capturing with DG discretization is such that $\forall v_h \in V_h, \ t \in (0, T]$

$$(\partial_t u_h, v_h) + a_h(u_h, v_h) + \sum_{K \in \mathcal{T}_h} \int_K r(u_h) v_h \, dx + a_{sc}(u_h, v_h) = l_h(v_h) + l_{sc}(v_h), \tag{3.7}$$

where

$$a_{sc}(u, v) = \sum_{K \in \mathcal{T}_h} \int_K \mu \nabla u \cdot \nabla v \, dx + \sum_{E \in \mathcal{E}_h^0 \cup \mathcal{E}_h^D} \int_E \{\!\{\mu \nabla u\}\!\} \cdot [\![v]\!] \, ds, \tag{3.8}$$

$$l_{sc}(v) = \sum_{E \in \mathcal{E}_h^N} \int_K \frac{\mu}{\varepsilon} g_N v \, ds. \tag{3.9}$$

Now, the main issue is to determine the value of the viscosity parameter μ. It is not wise to use a non-zero viscosity μ all across the solution domain since it is unnecessary in smooth regions. Therefore, one needs an indicator to identify the region where under- or overshoots are occurring. We will use the indicator introduced in [16]. This indicator is based on the rate of decay of expansion coefficients of the solution. For each element $K \in \mathcal{T}_h$, it can be described by

$$S_K = \frac{\|u - \hat{u}\|_{L^2(K)}^2}{\|u\|_{L^2(K)}^2}, \tag{3.10}$$

5

where u is the solution expressed in terms of p-th order of the orthogonal basis and $\hat{u}$ is a truncated expansion of the same solution, only containing the terms up to order $p-1$, i.e.,

$$u = \sum_{i=1}^{N(p)} u_i \varphi_i, \qquad \hat{u} = \sum_{i=1}^{N(p-1)} u_i \varphi_i,$$

where $\varphi_i \in V_h$, $i = 1, \cdots, N(p)$ are the basis polynomials. In [16] Persson et al. showed that S_K scales like $\sim 1/p^4$ by making a connection between the polynomial expansion and the Fourier expansion. Hence, they take the logarithm

$$s_K := \log_{10} S_K$$

to obtain a quantity that scales linearly with the decay exponent. Similarly, s_0 is expected to scale as $1/p^4$. Then, the amount of viscosity is taken to be constant over each element and determined by the following smooth function,

$$\mu_K = \begin{cases} 0, & \text{if } s_K < s_0 - \kappa, \\ \frac{\mu_0}{2}\left(1 + \sin \frac{\pi(s_K - s_0)}{2\kappa}\right), & \text{if } s_0 - \kappa \le s_K \le s_0 + \kappa, \\ \mu_0, & \text{if } s_K > s_0 + \kappa, \end{cases} \tag{3.11}$$

where μ_0 is the maximum viscosity, scaling with h/p and κ is the width of the activation "ramp". It is chosen empirically sufficiently large so as to obtain a sharp but smooth shock profile. Due to scaling with h/p, the amount of viscosity is of order $O(h/p)$ in order to resolve a shock. This means that the thinner or smaller extent shock is resolved when the higher order polynomials are used.

3.3. Time discretization

We use the θ-scheme [21] to discretize the problem (2.1) in time. Let N_T be a positive integer. The discrete time interval $\bar{I} = [0, T]$ is defined as

$$0 = t_0 < t_1 < \cdots < t_{N_T-1} < t_{N_T} = T$$

with size $k_n = t_n - t_{n-1}$ for $n = 1, \cdots, N_T$.

$$\left(\frac{u_h^n - u_h^{n-1}}{k_n}, v_h\right) + a_h(\theta u_h^n + (1-\theta)u_h^{n-1}, v_h)$$
$$+ \sum_{K \in \mathcal{T}_h} \int_K r(\theta u_h^n + (1-\theta)u_h^{n-1})v_h + a_{sc}(\theta u_h^n + (1-\theta)u_h^{n-1}, v_h)$$
$$= \theta\left(l_h^n(v_h) + l_{sc}^n(v_h)\right) + (1-\theta)\left(l_h^{n-1}(v_h) + l_{sc}^{n-1}(v_h)\right),$$

with the approximation of initial condition u_h^0.

4. Numerical Results

We have tested various single- and multi-component convection dominated problems with nonlinear reaction mechanisms. The penalty parameter σ in the SIPG method is chosen as $\sigma = 3p(p+1)$ on interior edges and $\sigma = 6p(p+1)$ on boundary edges. For time discretization, we use the method of Crack-Nicolson ($\theta = 0.5$). To solve (3.4) and (3.7), we use an inexact variant of Newton's method.

4.1. Example with u^2 reaction term in a single stationary case

This example taken from [1] is a stationary case with Dirichlet boundary conditions. The problem data are

$$\Omega = (0,1)^2, \quad \varepsilon = 10^{-8}, \quad \beta = \frac{1}{\sqrt{5}}(1,2)^T, \quad \alpha = 1 \quad \text{and} \quad r(u) = u^2.$$

The source function f and Dirichlet boundary conditions are chosen such that the exact solution is given by

$$u(x_1, x_2) = \frac{1}{2}\left(1 - \tanh\frac{2x_1 - x_2 - 0.25}{\sqrt{5\varepsilon}}\right),$$

which has an interior layer of thickness $O(\sqrt{\varepsilon}|\ln\varepsilon|)$ around $2x_1 - x_2 = \frac{1}{4}$.

h	dof	$p = 2$		dof	$p = 4$	
		SIPG	SIPG-SC		SIPG	SIPG-SC
1/2	48	1.28e-1	1.63e-1	120	1.13e-1	1.23e-1
1/4	192	8.85e-2	1.25e-1	480	5.39e-2	7.39e-2
1/8	768	6.56e-2	1.03e-1	1920	3.97e-2	6.49e-2
1/16	3072	5.02e-2	8.50e-2	7680	3.06e-2	5.33e-2
1/32	12288	3.78e-2	6.99e-2	30720	2.35e-2	4.36e-2
1/64	49152	2.83e-2	5.74e-2	122880	1.81e-2	3.51e-2

Table 1: Example 4.1: Mesh size h, number of degrees of freedom (dof) and errors in $\|\cdot\|_{L^2(\Omega)}$ without (SIPG) and with shock-capturing (SIPG-SC) for $p = 2, 4$, respectively.

Table 1 reveals the calculated errors in the $\|\cdot\|_{L^2(\Omega)}$ norm for the upwind SIPG approximation without and with shock capturing. Typically, the errors of the shock-capturing approach are even slightly larger than the errors of the upwind SIPG approach, which is due to the additional artificial cross-wind diffusion. However, spurious oscillations around the interior layer, where the derivative of the PDE solution is large, are reduced by the shock-capturing as shown in Figure 2. That means that the additional diffusion is located around the interior layer. Further, Figure 2 shows that the unphysical oscillations are almost gone when the higher order approximation ($p = 4$) is used for a fixed mesh size h.
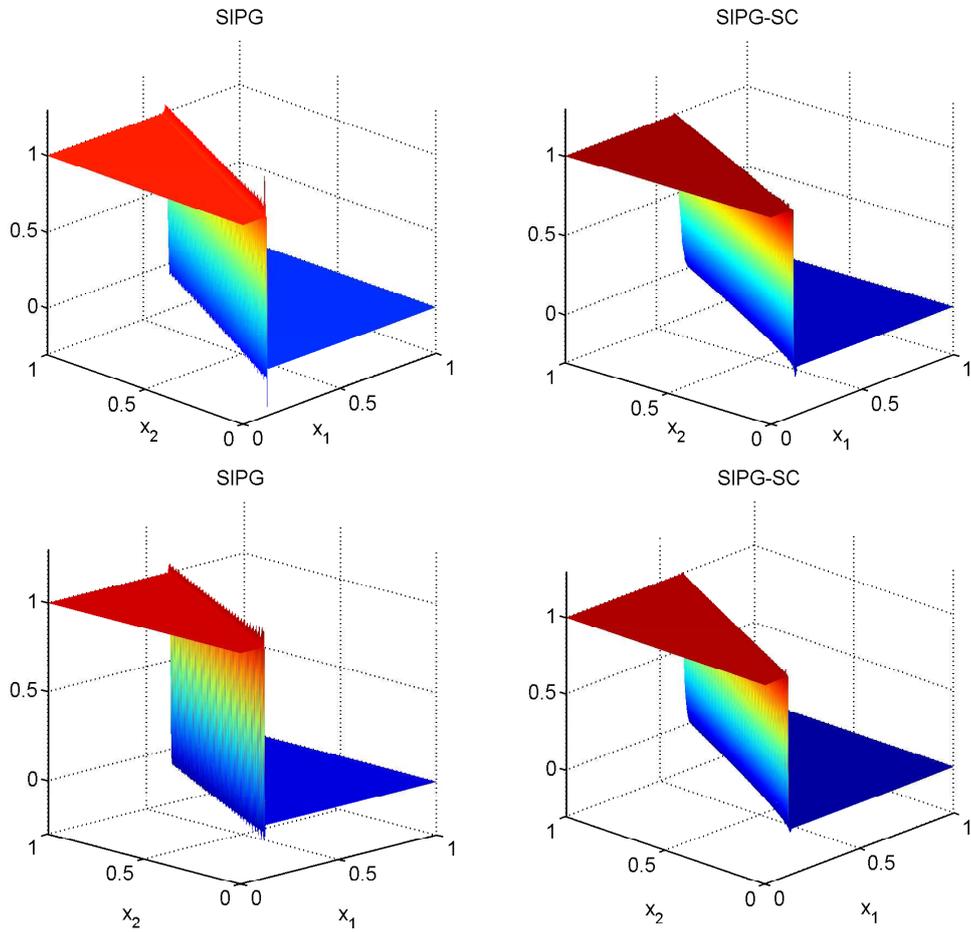
Figure 2: Example 4.1: The plots in the top row show the computed solutions without (SIPG) and with shock-capturing (SIPG-SC) for $p = 2$ and the plots on the bottom row show the computed solutions without (SIPG) and with shock-capturing (SIPG-SC) for $p = 4$ for a fixed mesh size $h = 1.56e - 2$.

4.2. Example with Monod-type reaction term in single stationary case

The following stationary example with unknown solution is taken from [1]. Let

$$\Omega = (0,1)^2, \quad \varepsilon = 10^{-8}, \quad \beta = (-x_2, x_1)^T, \quad \alpha = 1 \quad \text{and} \quad f = 0.$$

We have a Monod-type reaction rate $r(u) = -\frac{u}{1+u}$. The Dirichlet and Neumann boundary conditions are given by

$$g_D(x_1, x_2) = \begin{cases} 1, & \text{if } x_1 \in [1/3, 2/3] \text{ and } x_2 = 0, \\ 0, & \text{if } x_1 \in [0, 1/3] \cup (2/3, 1] \text{ and } x_2 = 0, \\ 0, & \text{if } x_1 = 1, \\ 0, & \text{if } x_2 = 1. \end{cases}$$

and

$$g_N(x_1, x_2) = 0 \quad \text{for} \quad x_1 = 0 \quad \text{and} \quad x_2 \in [0,1],$$

respectively.

The computed upwind SIPG solutions without and with shock-capturing are shown in Figure 3. The upwind SIPG solution has two interior layers that are resolved by using shock-capturing. The unphysical under- and over-shoots are almost eliminated when the higher polynomials ($p = 4$) are used.

4.3. Example with Arrhenius type reaction term in a single stationary case

The following stationary example taken from [10] models the jet diffusion flame in a combustor. The problem date is given by

$$\beta = (0.2, 0)^T, \quad \alpha = 0 \quad \text{and} \quad f = 0.$$

The nonlinear reaction term is an Arrhenius type given by

$$r(u, \gamma) = Au(c-u)e^{-E/d-u},$$

where c and d are known constants and the system parameters defined by $\gamma = (In A, E)$ can vary within the parameter domain $D : [5, 7.25] \times [0.05, 015]$. From a physical point of view, u represents fuel concentration, whereas $c - u$ is the concentration of the oxidizer. The parameters A and E are usually estimated from experimental data. Figure 4 shows the 2D combustor domain. The Dirichlet boundary conditions at the left vertical boundary of the domain are given by

$$g_D(x_1, x_2) = \begin{cases} 0, & \text{if } 0 \le x_2 < 3 \text{ mm}, \\ c, & \text{if } 3 \le x_2 < 6 \text{ mm}, \\ 0, & \text{if } 6 \le x_2 \le 9 \text{ mm}. \end{cases}$$

All other boundaries have homogeneous Neumann boundary conditions.
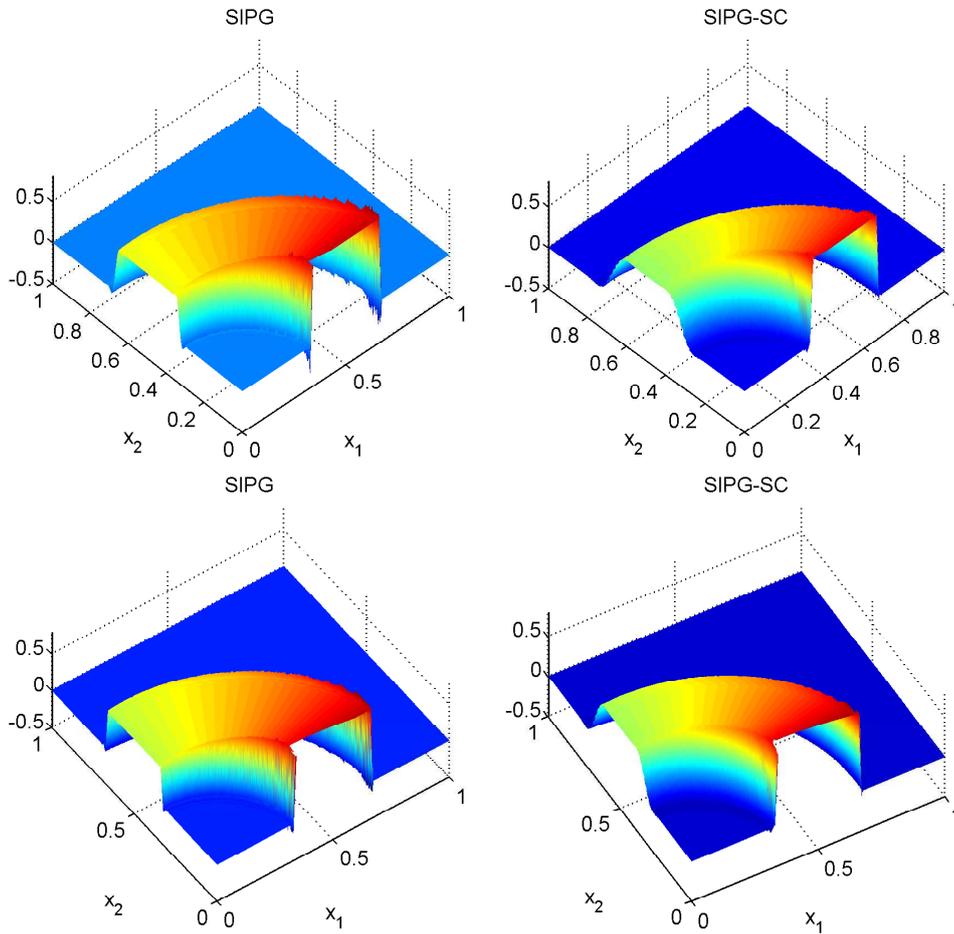
Figure 3: Example 4.2: The plots in the top row show the computed solutions without (SIPG) and with shock-capturing (SIPG-SC) for $p = 2$ and the plots on the bottom row show the computed solutions without (SIPG) and with shock-capturing (SIPG-SC) for $p = 4$ for a fixed mesh size $h = 1.56e - 2$.
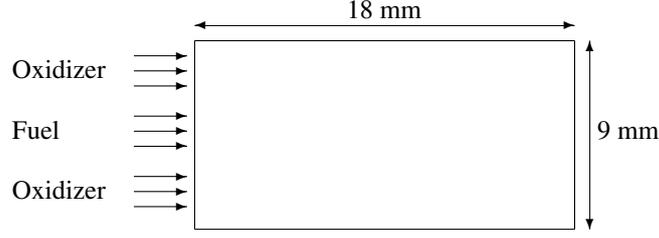
Figure 4: The domain for the modelled fuel concentration problem.

We have tested the Example 4.3 with various $\gamma = (\ln A, E)$ parameters for $\varepsilon = 5 \times 10^{-6}$ in Figure 5. The results show that the upwind SIPG discretization works well. However, when we consider smaller diffusion parameter $\varepsilon = 5 \times 10^{-7}$, the unphysical oscillations occur, see Figure 6. By applying shock-capturing we handle these spurious oscillations.
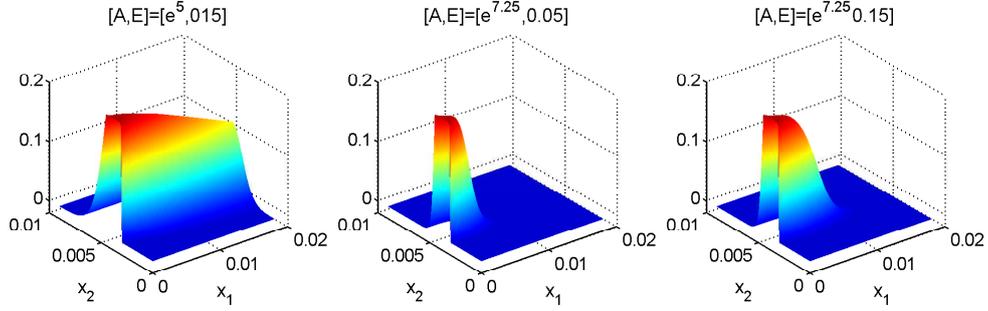
Figure 5: Example 4.3: Computed SIPG solutions for various $\gamma = (\ln A, E)$ parameters with $p = 2$, $h = 1.56e - 2$ and $\varepsilon = 5 \times 10^{-6}$.

4.4. Example with u^4 reaction term in a single nonstationary case

We now study the unsteady problem with Dirichlet boundary conditions taken from [3]. Let

$$\Omega = (0,1)^2, \quad \varepsilon = 10^{-6}, \quad \beta = (2,3)^T, \quad \alpha = 0, \quad T = 1 \quad \text{and} \quad r(u) = u^4.$$

The source function f and Dirichlet boundary conditions are chosen such that the exact solution is given by

$$u(x_1, x_2, t) = 16 \sin(\pi t) x_1 (1 - x_1) x_2 (1 - x_2)$$
$$\times \left[\frac{1}{2} + \frac{1}{\pi} \arctan \left(\frac{2}{\sqrt{\varepsilon}} \left(\frac{1}{16} - (x_1 - 0.5)^2 - (x_2 - 0.5)^2 \right) \right) \right],$$

which has a circular interior layer of characteristic width $\sqrt{\varepsilon}$.

11
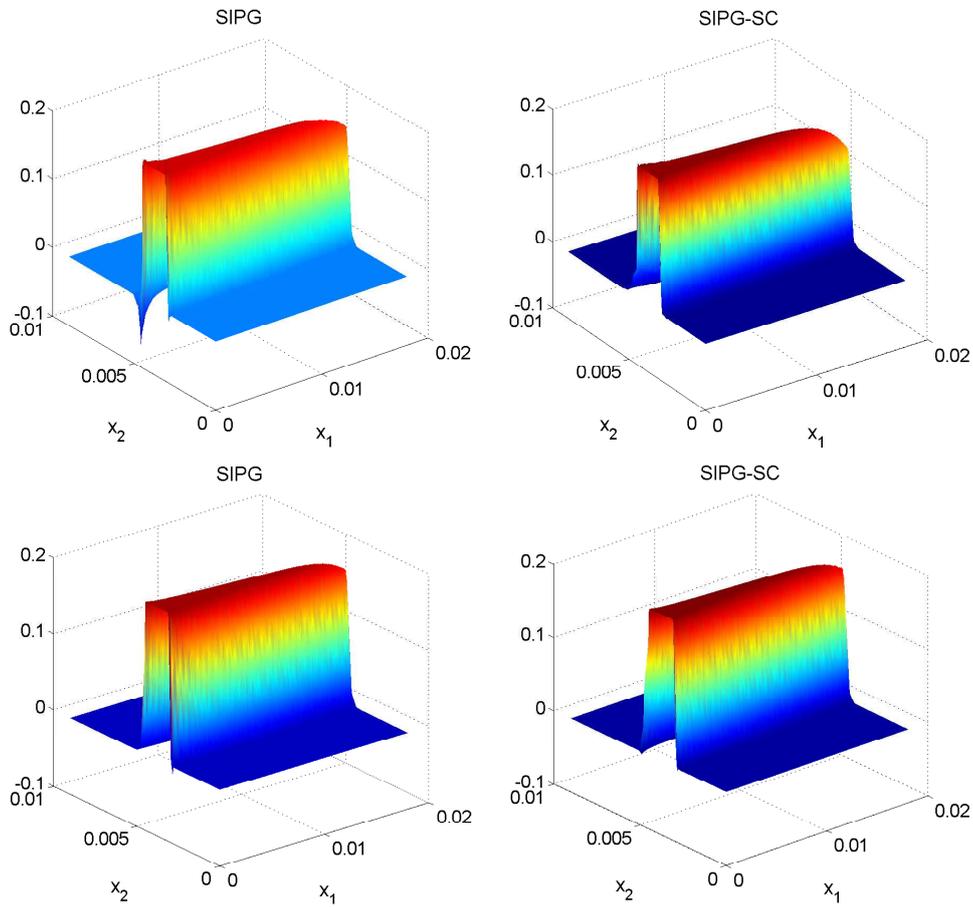
Figure 6: Example 4.3: The plots in the top row show the computed solutions without (SIPG) and with shock-capturing (SIPG-SC) for $p = 4$ and the plots on the bottom row show the computed solutions without (SIPG) and with shock-capturing (SIPG-SC) for $p = 6$ for a fixed mesh size $h = 3.125e - 2$, $\varepsilon = 5 \times 10^{-7}$ and $\gamma = [e^{7.25}, 0.15]$.

Figure 7 reveals the computed numerical solutions without and with shock-capturing by using quadratic polynomials with time step size $k = 10^{-2}$. Although the upwind SIPG approximation yields some oscillations, these oscillations are reduced after shock-capturing.
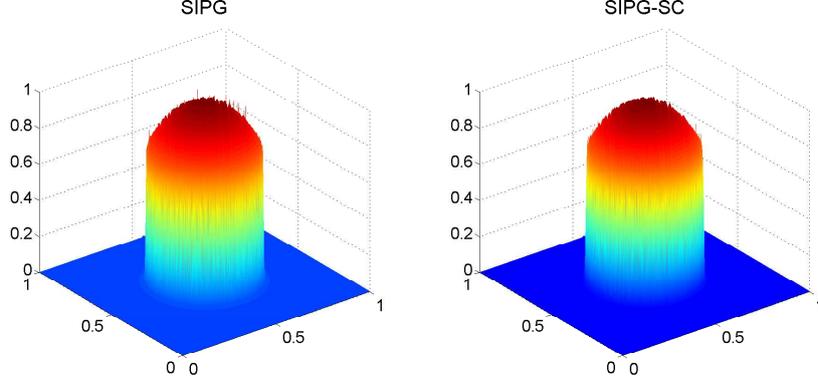
Figure 7: Example 4.4: The plots show the computed solutions without (SIPG) and with shock-capturing (SIPG-SC) for $p = 2$ with $h = 1.56e - 2$ at $t = 0.5$.

4.5. Example with Arrhenius type reaction term in a coupled stationary case

The following stationary coupled system with unknown solution is a modified form of the example studied in [20].

$$-\varepsilon \Delta u + \beta \cdot \nabla u - (\Delta H/(\rho u_p)) k_0 v e^{-(E/Ru)} = 0 \qquad \text{in } \Omega,$$

$$-\varepsilon \Delta v + \beta \cdot \nabla v + k_0 v e^{-(E/Ru)} = 0 \qquad \text{in } \Omega.$$

The Dirichlet and Neumann boundary conditions are defined by

13

The problem data is

$$\Omega = [0,1]^2, \quad \varepsilon = 10^{-6}, \quad \beta = (1 - x_2^2, 0),$$
$$k_0 = 3 \times 10^8, \quad \Delta H / (\rho u_p) = 100 \quad \text{and} \quad E/R = 10^4.$$

Here, we solve a coupled convection dominated problem with Arrhenius nonlinear expression, consisting of the product of a concentration of chemical component and an exponential function of the temperature. The computed solutions without shock-capturing exhibit high oscillations when the quadratic polynomials are used. However, these unphysical oscillations are reduced with shock-capturing, see Figure 8. Figure 9 shows the numerical approximations for the higher order polynomials ($p = 4$). Similarly to previous examples, the higher order approximations produce better results.

5. Conclusions

We have solved convection dominated reaction-diffusion problems with various nonlinear reaction terms by using the upwind symmetric interior penalty Galerkin (SIPG) method. A shock-capturing method with a discontinuity detection strategy has been used in order to eliminate unphysical oscillations caused by the boundary and/or interior layers and nonlinear reaction terms. As a future work, combination of hp-adaptivity with shock-capturing can be addressed to narrow the shock layers.

References

[1] M. Bause. Stabilized finite element methods with shock-capturing for nonlinear convectiondiffusion-reaction models. In *Numerical Mathematics and Advanced Applications 2009*, pages 125–133. Springer Berlin Heidelberg, 2010.

[2] M. Bause and P. Knabner. Numerical simulation of contaminant biodegradation by higher order methods and adaptive time stepping. *Comput. Visul. Sci.*, 7:61–78, 2004.

[3] M. Bause and K. Schwegler. Analysis of stabilized higher-order finite element approximation of nonstationary and nonlinear convection-diffusion-reaction equations. *Comput. Methods Appl. Mech. Engrg.*, 209-212:184–196, 2012.

[4] A. Cangiani, J. Chapman, E. H. Georgoulis, and M. Jensen. On local super-penalization of interior penalty discontinuous galerkin methods. *CoRR*, abs/1205.5672, 2012.

[5] B. Cockburn. On discontinuous Galerkin methods for convection–dominated problems. In A. Quarteroni, editor, *Advanced Numerical Approximation of Nonlinear Hyperbolic Equations*, Lecture Notes in Mathematics, Vol. 1697, pages 151–268. Springer Verlag, 1998.

[6] B. Cockburn, S. Hou, and C.-W. Shu. TVD Runge–Kutta local projection discontinuous Galerkin finite element method for scalar conservation laws IV: The multidimensional case. *Math. Comp.*, 54:545–581, 1990.
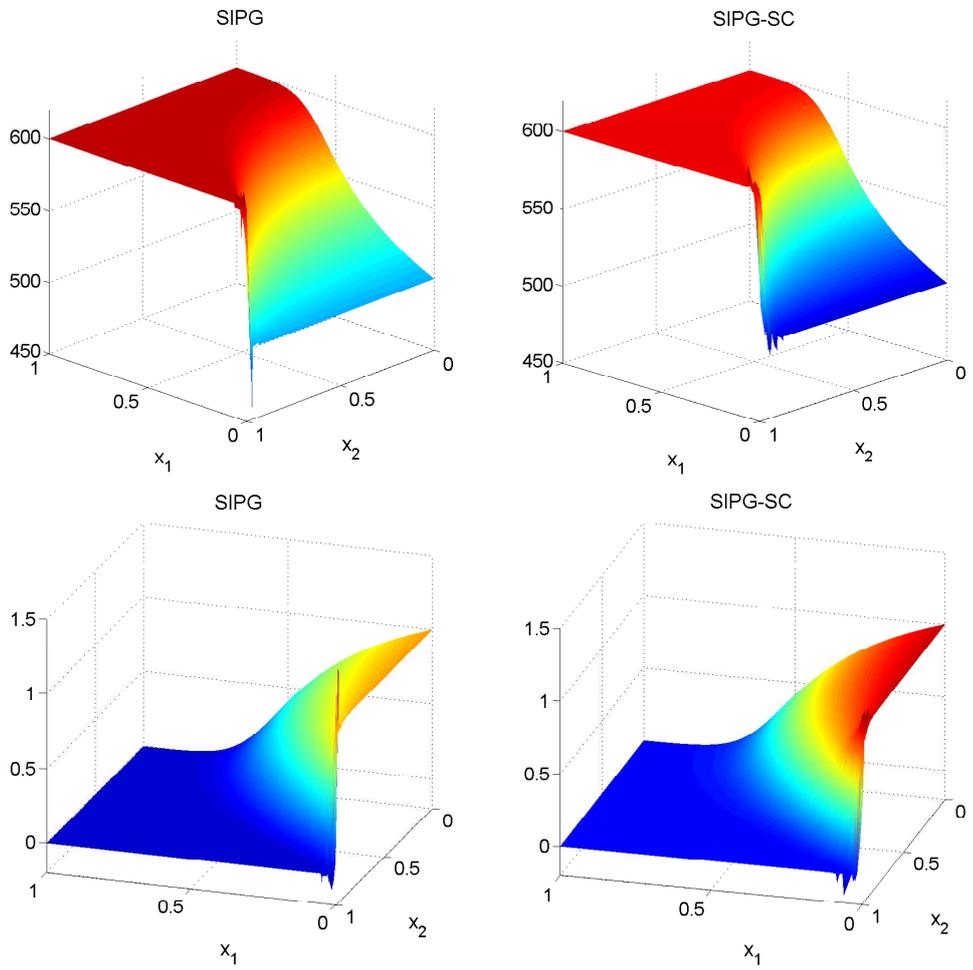
Figure 8: Example 4.5: The plots in the top row show the computed solutions without (SIPG) and with shock-capturing (SIPG-SC) for unknown *u* and the plots on the bottom row show the computed solutions without (SIPG) and with shock-capturing (SIPG-SC) for unknown *v* using $p = 2$ with 12288 dof.
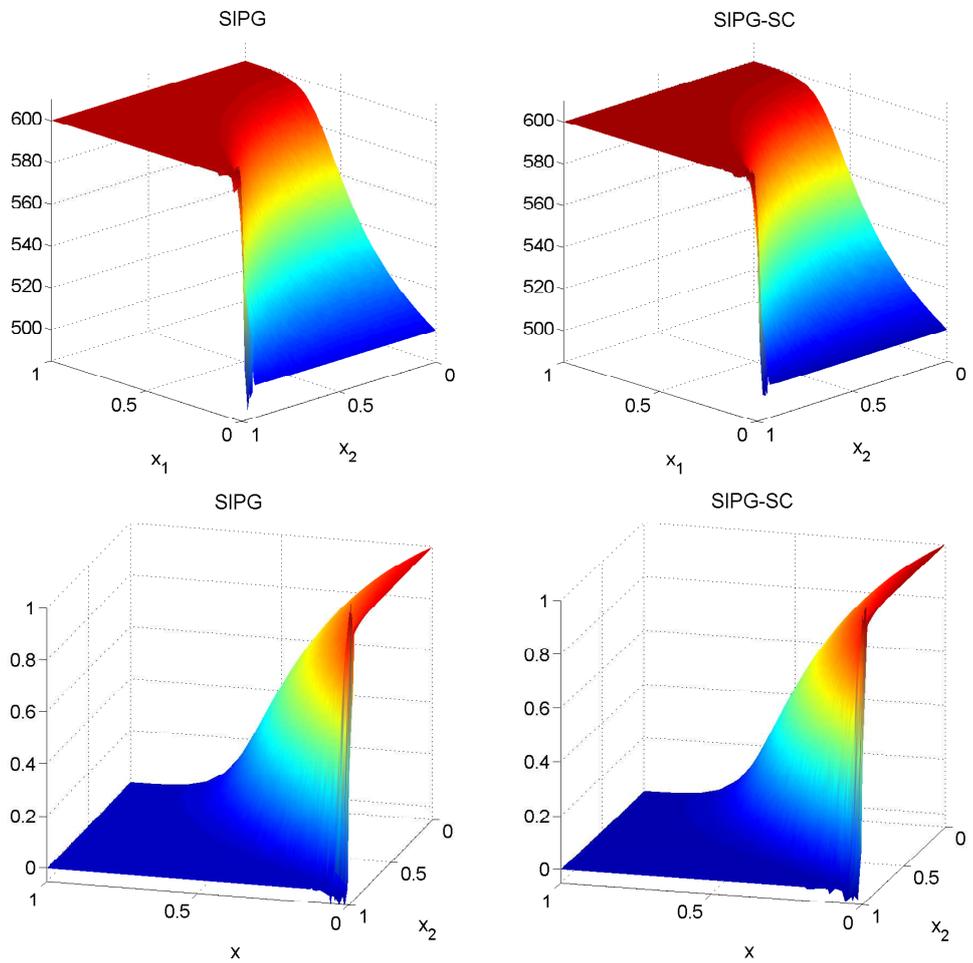
Figure 9: Example 4.5: The plots in the top row show the computed solutions without (SIPG) and with shock-capturing (SIPG-SC) for unknown u and the plots on the bottom row show the computed solutions without (SIPG) and with shock-capturing (SIPG-SC) for unknown v using $p = 4$ with 7680 dof.

[7] B. Cockburn and C.-W. Shu. TVD Runge–Kutta local projection discontinuous Galerkin finite element method for scalar conservation laws II: General framework. *Math. Comp.*, 52:411–435, 1989.

[8] B. Cockburn and C.-W. Shu. Runge-Kutta discontinuous Galerkin methods for convection-dominated problems. *J. Sci. Comput.*, 16(3):173–261, 2001.

[9] H. C. Elman, D. J. Silvester, and A. J. Wathen. *Finite Elements and Fast Iterative Solvers with Applications in Incompressible Fluid Dynamics*. Oxford University Press, Oxford, 2005.

[10] D. Galbally, K. Fidkowski, K. Willcox, and O. Ghattas. Nonlinear model reduction for uncertainty quantification in large-scale inverse problems. *Internat. J. Numer. Methods Engrg.*, 81(12):1581–1603, 2010.

[11] R. Helmig. *Multiphase Flow and Transport Processes in the Subsurface*. Springer, Berlin, 1997.

[12] R. Helmig. *Combustion: Physical and Chemical Modelling and Simulation, Experiments, Pollutant Formation*. Springer, Berlin, 2009.

[13] P. Houston, C. Schwab, and E. Süli. Discontinuous *hp*-finite element methods for advection-diffusion-reaction problems. *SIAM J. Numer. Anal.*, 39(6):2133–2163 (electronic), 2002.

[14] V. John and E. Schmeyer. Finite element methods for time-dependent convection-diffusion-reaction equations with small diffusion. *Comput. Methods Appl. Mech. Engrg*, 198(3-4):475 – 494, 2008.

[15] A. Lapidus. A detached shock calculation by second-order finite differences. *J. Computational Phys.*, 2(2):154–177, 1967.

[16] P. Persson and J. Peraire. Sub-cell shock capturing for discontinuous galerkin methods. In *Proc. of the 44th AIAA Aerospace Sciences Meeting and Exhibit*, volume 112, 2006.

[17] J. Qiu and C. W. Shu. Runge-kutta discontinuous galerkin method using weno limiters. *SIAM J. Sci. Comput.*, 26(3):907–929, 2005.

[18] B. Rivière. *Discontinuous Galerkin methods for solving elliptic and parabolic equations. Theory and implementation*, volume 35 of *Frontiers in Applied Mathematics*. Society for Industrial and Applied Mathematics (SIAM), Philadelphia, PA, 2008.

[19] D. Schötzau and L. Zhu. A robust a-posteriori error estimator for discontinuous Galerkin methods for convection-diffusion equations. *Appl. Numer. Math.*, 59(9):2236–2255, 2009.

[20] T.E. Tezduyar and Y.J. Park. Discontinuity capturing finite element formulations for nonlinear convection-diffusion-reaction problems. *Comput. Methods Appl. Mech. Engrg.*, 59:307–325, 1986.

[21] J. W. Thomas. *Numerical Partial Differential Equations: Finite Difference Methods.* Texts in Applied Mathematics. Vol. 22. Springer, Berlin, New York, 1995.

[22] J. von Neumann and R.D. Richtmyer. A method for numerical calculation of hydro dymamic shocks. *J. Appl. Phys.*, 21:232–237, 1950.

A. Preliminaries for Sobolev spaces

In this Appendix, we give the definitions of some Sobolev and functional spaces used along this paper.

The vector space $L^p(\Omega)$ is defined by

$$L^p(\Omega) = \{v \text{ Lebesgue measurable} : \|v\|_{L^p(\Omega)} < \infty\}$$

with the following L^p norm:

$$\|v\|_{L^p(\Omega)} = \left(\int_\Omega |v|^p\right)^{1/p}.$$

The space $L^\infty(\Omega)$ is the space of bounded functions:

$$L^\infty(\Omega) = \{v : \|v\|_{L^\infty(\Omega)} < \infty\} \quad \text{with} \quad \|v\|_{L^\infty(\Omega)} = \operatorname{ess\,sup}\{|v(x)| : x \in \Omega\}.$$

Let $D(\Omega)$ denote the space of C^∞ functions. The dual space $D'(\Omega)$ is called the space of distributions. For any multi-index $\alpha = (\alpha_1, \cdots, \alpha_d) \in \mathbb{N}^d$ and $|\alpha| = \sum_{i=1}^d \alpha_i$, the distributional derivative $D^\alpha v \in D'(\Omega)$ is defined by

$$D^\alpha v(\phi) = (-1)^{|\alpha|} \int_\Omega v(x) \frac{\partial^{|\alpha|}\phi}{\partial x_1^{\alpha_1} \cdots \partial x_d^{\alpha_d}}, \qquad \forall \phi \in D(\Omega).$$

Then, we introduce the Sobolev space $W^{k,p}(\Omega)$:

$$W^{k,p}(\Omega) = \{v \in L^p(\Omega) : D^\alpha v \in L^p(\Omega) \ \forall |\alpha| \le k\}$$

equipped with the norm

$$\|v\|_{W^{k,p}(\Omega)} = \left(\sum_{|\alpha| \le k} \|D^\alpha v\|_{L^p(\Omega)}^p\right)^{1/p}, \quad p \in [1, \infty),$$

$$\|v\|_{W^{k,\infty}(\Omega)} = \sum_{|\alpha| \le k} \|D^\alpha v\|_{L^\infty(\Omega)}.$$

Moreover, $H^k(\Omega) = W^{k,2}(\Omega)$ is called Hilbert space. Let us now define the the Sobolev spaces with fractional indices which are necessary to define the spaces for boundary conditions. The space $H^{k+1/2}(\Omega)$ with k integer is obtained by interpolating between the spaces $H^k(\Omega)$ and $H^{k+1}(\Omega)$.

Finally, we consider the space of functions mapping the time interval $(0,T)$ to a normed space X for $r \geq 1$,

$$L^r(0,T;X) = \{z : [0,T] \to X \text{ measurable} : \int_0^T \|z(t)\|_X^r \, dt < \infty\},$$

with the norm $\|\cdot\|_X$

$$\|z(t)\|_{L^r(0,T;X)} = \begin{cases} \left(\int_0^T \|z(t)\|_X^r \, dt\right)^{1/r}, & \text{if } 1 \leq r < \infty, \\ \underset{t \in (0,T]}{\text{ess sup}} \ \|z(t)\|_X, & \text{if } r = \infty. \end{cases}$$